Electronic Supplementary Material

Reduction kinetics of $SrFeO_{3-\delta}$/CaO·MnO nanocomposite as effective oxygen carrier for chemical looping partial oxidation of methane

Xinhe Wang[1], Liuqing Yang[2], Xiaolin Ji[2], Yunfei Gao[3,4], Fanxing Li[4], Junshe Zhang (✉)[2], Jinjia Wei (✉)[1,2]

1 State Key Laboratory of Multiphase Flow in Power Engineering, Xi'an Jiaotong University, Xi'an 710049, China

2 School of Chemical Engineering and Technology, Xi'an Jiaotong University, Xi'an 710049, China

3 Institute of Clean Coal Technology, East China University of Science and Technology, Shanghai 200237, China

4 Department of Chemical and Biomolecular Engineering, North Carolina State University, Raleigh, NC 27695, USA

E-mails: jzhang08@xjtu.edu.cn (Zhang J); jjwei@mail.xjtu.edu.cn (Wei J)

Table S1. Solid-state rate and integral expressions for different reaction models [1]

Model / Mechanism	Differential form $f(X)=1/k\,dX/dt$	Integral form $g(X)=kt$
Nucleation models		
Power law (P2)	$2X^{1/2}$	$X^{1/2}$
Power law (P3)	$3X^{2/3}$	$X^{1/3}$
Power law (P4)	$4X^{3/4}$	$X^{1/4}$
Avrami-Erofeyev (A2)	$2(1-X)[-\ln(1-X)]^{1/2}$	$[-\ln(1-X)]^{1/2}$
Avrami-Erofeyev (A3)	$3(1-X)[-\ln(1-X)]^{2/3}$	$[-\ln(1-X)]^{1/3}$
Avrami-Erofeyev (A4)	$4(1-X)[-\ln(1-X)]^{3/4}$	$[-\ln(1-X)]^{1/4}$
Prout-Tompkins (B1)	$X(1-X)$	$\ln[X/(1-X)]+c^{n}$
Geometrical contraction models		
Contracting area (R2)	$2(1-X)^{1/2}$	$1-(1-X)^{1/2}$
Contracting area (R3)	$3(1-X)^{2/3}$	$1-(1-X)^{1/3}$
Diffusion models		
1-D diffusion (D1)	$1/(2X)$	X^{2}
2-D diffusion (D2)	$-[1/\ln(1-X)]$	$((1-X)\ln(1-X))+X$
3-D diffusion-Jander (D3)	$[3(1-X)^{2/3}]/[2(1-(1-X)^{1/3})]$	$(1-(1-X)^{1/3})^{2}$
Ginstling-Brounshtein (D4)	$3/[2((1-X)^{-1/3}-1)]$	$1-(2/3)X-(1-X)^{2/3}$
Reaction-order models		
Zero-order (F0/R1)	1	X
First-order (F1)	$1-X$	$-\ln(1-X)$
Second-order (F2)	$(1-X)^{2}$	$[1/(1-X)]-1$
Third-order (F3)	$(1-X)^{3}$	$(1/2)[(1-X)^{-2}-1]$

Table S2. Comparison of the activation energy reported in the literature

Redox materials	Temperature range	Experimental method	*Ea* (kJ/mol)	Ref.
10%Co/mesoporous alumina	973–1073 K	Isothermal TCD	43.48	[2]
$Sr_{2.45}La_{0.55}FeCoO_{7-\delta}$	1073-1173 K	Isothermal GC	58.3	[3]
$NiO/MgAl_2O_4$	1073–1273 K	Isothermal TGA	114	[4]
$SrFeO_{3-\delta}$-CaO•MnO	1123~1223 K	Isothermal TGA	59.8	This work

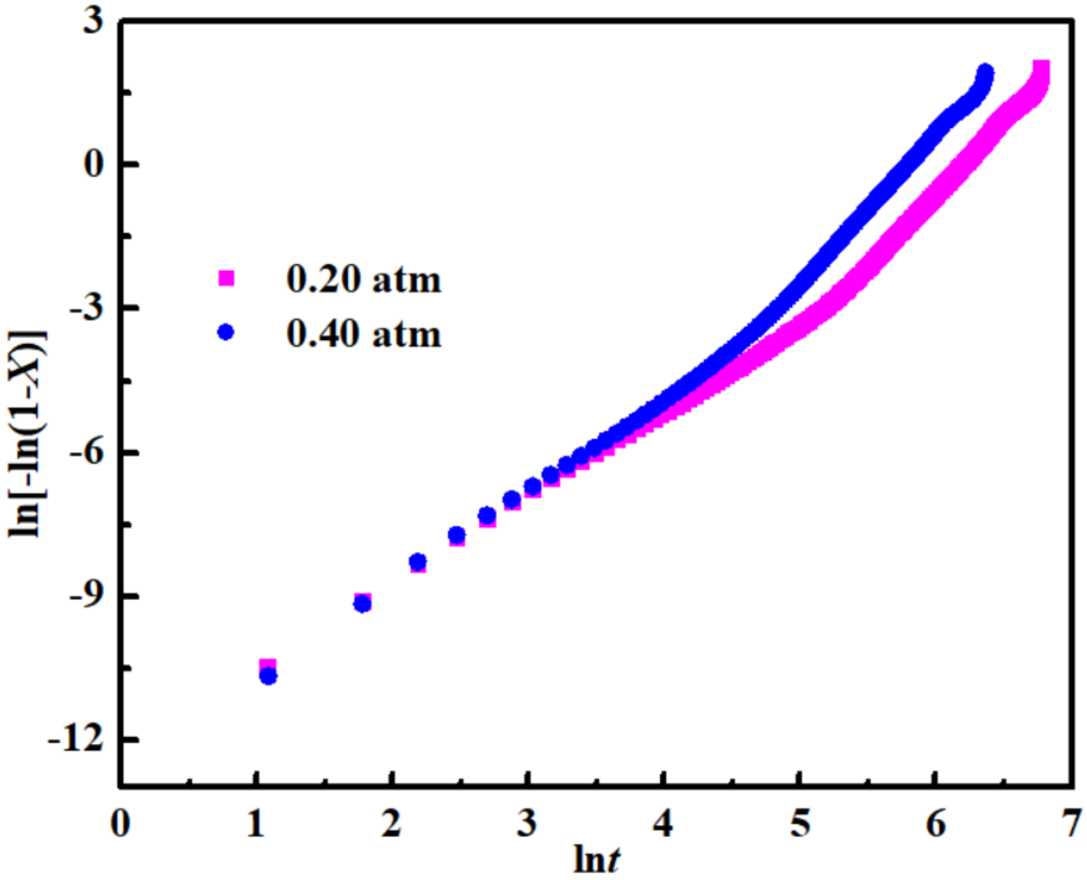

Fig. S1. The plots of ln[-ln(1-X)] as function of time *t* for two methane pressures,

Reaction conditions: m_{SF-CM} = 1 g, T = 900 °C, F=110 STP mL/min, P =1 atm.

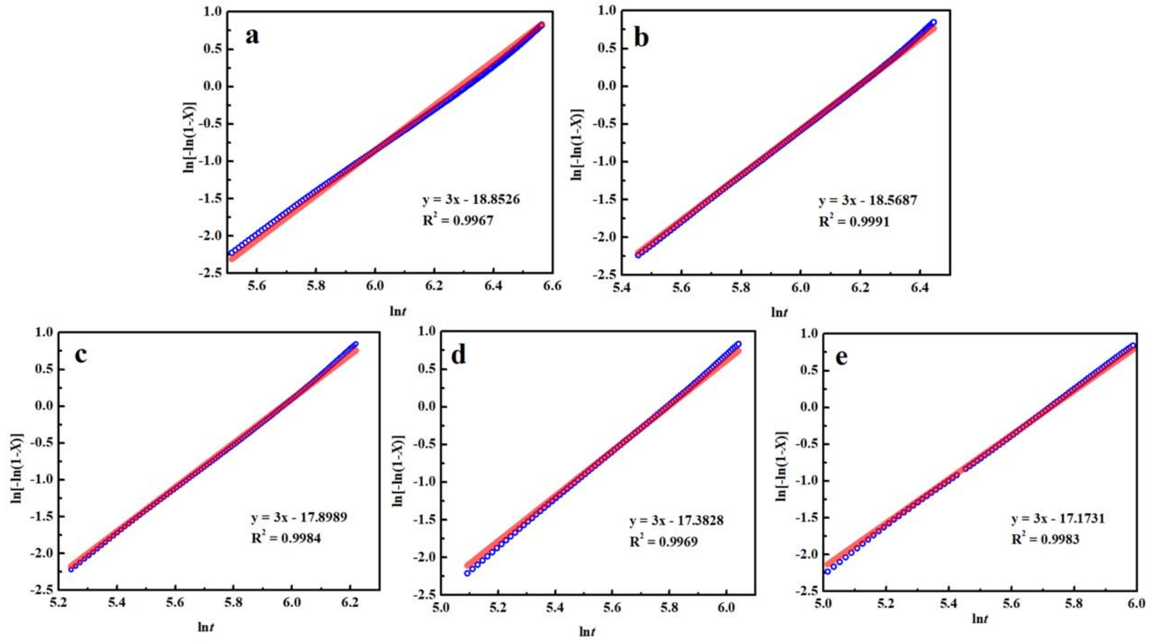

Fig. S2. The plots of ln[-ln(1-*X*)] vs. ln*t* for five methane pressures: (a) 0.15 atm, (b) 0.20 atm, (c) 0.30 atm, (d) 0.40 atm, (e) 0.50 atm. Reaction conditions: $m_{\text{SF-CM}}$ = 1 g, *T* = 900 °C, *F*=110 STP mL/min, *P*=1 atm.

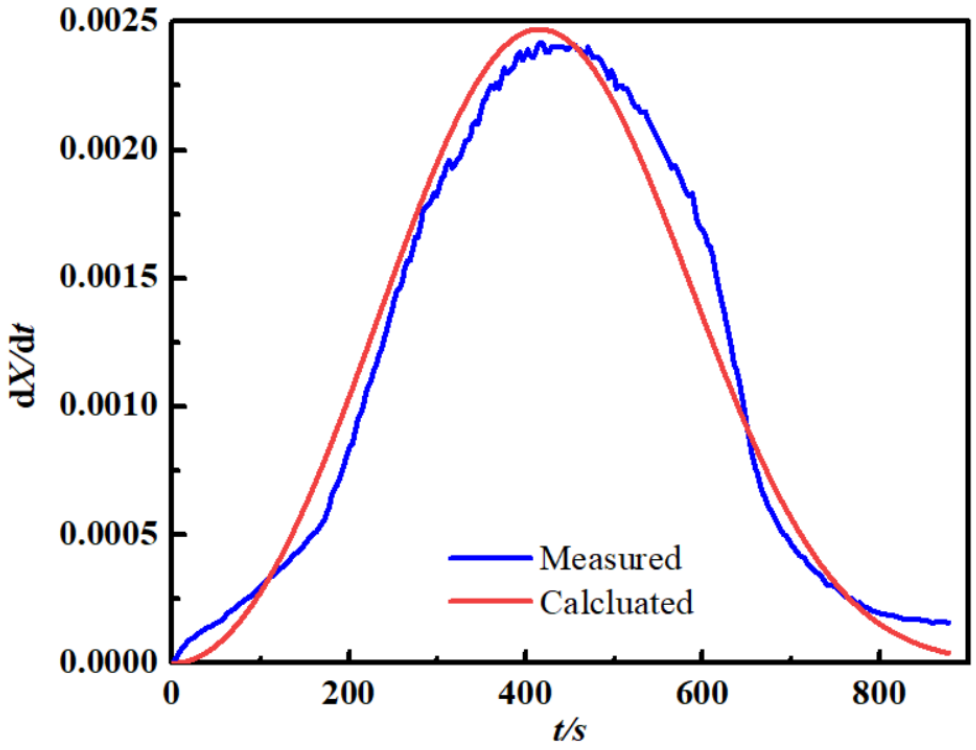

Fig. S3. The predicted and measured reduction rates for a methane partial pressure of 0.20 atm. Reaction conditions: $m_{\mathrm{SF\text{-}CM}}$ =1 g, T=900 °C, F=110 STP mL/min, P=1 atm.

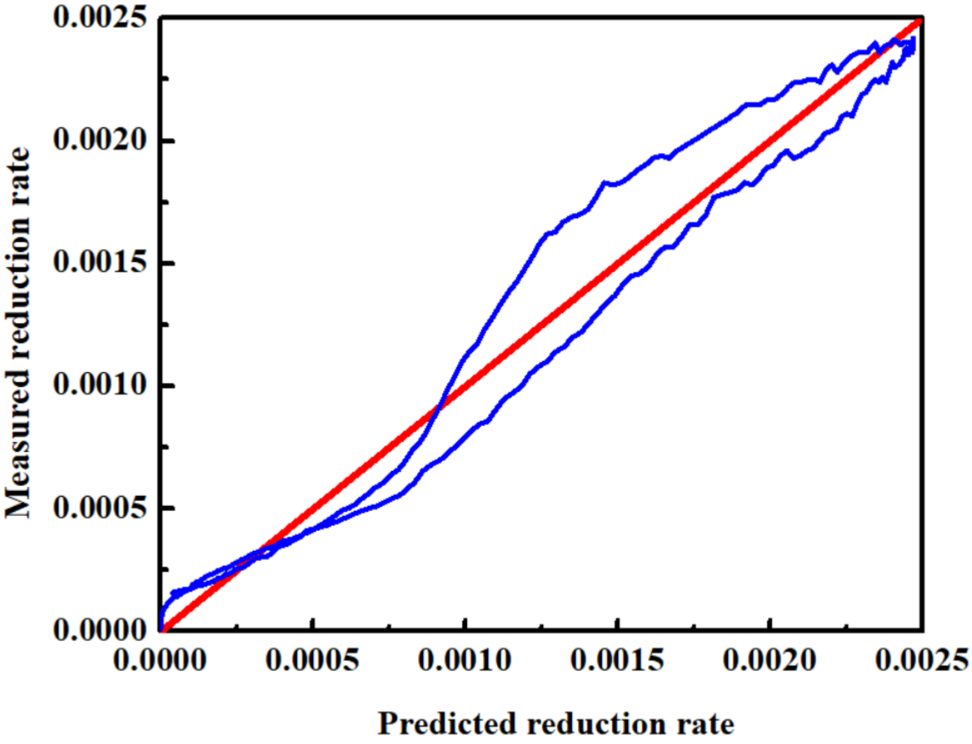

Fig. S4. The Q-Q plot for a methane patial pressure of 0.20 atm. Reaction conditions: $m_{\mathrm{SF\text{-}CM}}$ =1 g, T=900 °C, F=110 STP mL/min, P=1 atm.

References

1. Khawam A, Flanagan DR. Solid-state kinetic models: basics and mathematical fundamentals, The Journal of Physical Chemistry B, 2006, 110(35): 17315-28

2. Tran NT, Van Le Q, Van Cuong N, Nguyen TD, Huy Phuc NH, Phuong PTT, Monir MU, Aziz AA, Truong QD, Abidin SZ, Nanda S, Vo DVN. La-doped cobalt supported on mesoporous alumina catalysts for improved methane dry reforming and coke

mitigation. Journal of the Energy Institute, 2020, 93(4):1571-1580

3. Kagomiya I, Suzumura M, Kakimoto Ki, Ohsato H. Influence of Layered Perovskite Structure on Oxygen Permeability of Sr–La–Fe–Co Oxide. Journal of the Physical Society of Japan, 2010,79: 109-112

4. Zafar Q, Abad A, Mattisson T, Gevert B. Reaction Kinetics of Freeze-Granulated NiO/$MgAl_2O_4$ Oxygen Carrier Particles for Chemical-Looping Combustion. Energy & Fuels, 2007, 21(2): 610-618